

Multimodal Ocular Biometrics Approach: A Feasibility Study

Oleg V. Komogortsev¹, Alexey Karpov¹, Corey D. Holland¹, Hugo P. Proença²
Texas State University – San Marcos¹, University of Beira Interior²
Department of Computer Science
ok11@txstate.edu, ak26@txstate.edu, ch1570@txstate.edu, hugomcp@di.ubi.pt

Abstract

Growing efforts have been concentrated on the development of alternative biometric recognition strategies, the intended goal to increase the accuracy and counterfeit-resistance of existing systems without increased cost. In this paper, we propose and evaluate a novel biometric approach using three fundamentally different traits captured by the same camera sensor. Considered traits include: 1) the internal, non-visible, anatomical properties of the human eye, represented by Oculomotor Plant Characteristics (OPC); 2) the visual attention strategies employed by the brain, represented by Complex Eye Movement patterns (CEM); and, 3) the unique physical structure of the iris. Our experiments, performed using a low-cost web camera, indicate that the combined ocular traits improve the accuracy of the resulting system. As a result, the combined ocular traits have the potential to enhance the accuracy and counterfeit-resistance of existing and future biometric systems.

1. Introduction

Biometric systems are becoming increasingly more important to advance security in a wide variety of applications, including everyday computer access, health care, information systems, e-commerce, and border control. Multimodal biometric systems often rely on traits such as iris pattern, fingerprints, face, hand geometry, and voice [1]. While the security potential of biometric techniques is high, unsolved security challenges continue to escalate with recent technological advances that allow the production of high quality artifacts [2] and sophisticated spoofing mechanisms [3].

Multimodal biometric systems often provide increased accuracy of identification and resistance to spoofing in comparison to single-trait systems [1]; however, these benefits come at the expense of decreased usability and increased cost, due largely to the employment of multiple sensors and additional steps in the data acquisition process.

In this work, we investigate the feasibility of a multimodal ocular biometrics approach which uses the infor-

mation from three fundamentally different physiological and behavioral traits, and requires the use of only a single image sensor and an array of infrared (IR) lights. Considered traits include: 1) the internal, non-visible, anatomical properties of the human eye, represented by Oculomotor Plant Characteristics (OPC); 2) the visual attention strategies employed by the brain, represented by Complex Eye movement patterns (CEM); and, 3) the unique physical structure of the iris. OPC and CEM traits are inferred from the dynamics of eye movements derived from the sequence of eye images captured by the sensor, while the iris pattern is extracted directly from the same images. The combination of accurate static traits, such as iris patterns, and highly dynamic traits, such as eye movements, has the potential to provide a high degree of identification accuracy and counterfeit-resistance to the underlying system.

This work contributes to the state-of-the-art by: 1) investigating the performance of both individual and combined CEM-, OPC-, and iris-based biometrics on a single, low-cost image sensor; 2) generate the largest existing eye movement database for biometric research.

This paper is organized as follows: Section 2 discusses the state-of-the-art in related research directions and outlines the contribution of our work to the existing body of knowledge, Section 3 presents architectures of the multimodal ocular biometrics, Section 4 describes experimental setup, Section 5 presents experimental results, and Sections 6 and 7 include the discussion and conclusion, respectively.

2. Related Work

2.1. Eye Movement-driven Biometrics

The human eye exhibits several basic types of eye movement in response to various stimuli (both internal and external). In the field of human-computer interaction, fixations and saccades are of primary interest. Fixations occur when the eye globe is held in a relatively stable position such that the fovea remains centered on an object of interest, providing heightened visual acuity. Saccades occur when the eye globe rotates quickly between points of fixation, with very little visual acuity maintained during rotation. The term scanpath refers to the spatial path formed by a sequence of fixations and saccades.

Kasprowski and Ober [4] employed the uncalibrated positional signal captured by a custom-made eye tracking in a verification scenario. The signal was processed by Naïve Bayes, C45 Decision Tree, SVM polynomial, and KNN (k=3, 7) algorithms. The visual stimulus was presented as a sequence of jumping dots, and data was captured for 8 sec at a frequency of 250 Hz. The best reported result provided HTER = 12% (FAR = 1.48%, FRR = 22.59%), obtained from 9 subjects. Subsequently in [5], the authors extended their research by working with features such as average velocity direction, eye distance to stimulus, distance between eyes, and features extracted from discrete Fourier and wavelet transforms. The resulting feature vectors were merged by voting method for an average HTER of 3.88-11.25%; however, the authors did not report the number of subjects considered.

Bednarik et al. [6] employed such metrics as pupil diameter/dilation, eye velocity, and distance between eyes captured by a commercial Tobii ET-1750 eye tracking system in an identification scenario. Metrics were processed via Fourier spectrum, principal component analysis, and a combination of the two. The visual stimulus was a centrally positioned cross, displayed for a period of 1 sec, and data was captured for 12 subjects with a sampling frequency of 50 Hz. For each subject, data was captured during a single recording session, and the best reported result yielded an identification rate of 92%, obtained by weighted fusion of the three metrics.

Kinnunen et al. [6] employed information about the angles the eye travels within a temporal window, captured by a commercial Tobii X120 eye tracking system in a verification scenario. Captured information was processed into features by a Gaussian mixture model, enhanced by a universal background model. The visual stimulus was a 25 min comedy video, and data was captured for 17 subjects with a sampling frequency of 120 Hz. Each subject viewed two videos, one of which was employed for enrollment and the other for verification. The best reported result yielded an HTER of 29.4%, obtained by weighted fusion.

Rigas et al. [7] investigated a method in which a sequence of fixations and saccades was represented by a minimum spanning tree (MST). MST templates were compared by a statistical test designed to extract mean and variance. The visual stimulus was a set of facial images, with a total of 10 images presented during each recording session for 4 sec each. Each subject participated in 8 recording sessions over two days, and data was collected by a Dual Purkinje eye tracking system with a sampling rate of 50 Hz. EER was reported at 30%.

Komogortsev et al. [8] proposed a method of authentication via oculomotor plant characteristics (OPC) estimated from eye movements, with obtained OPC templates compared by Hotelling's T-square test. The visual stimulus was presented as a jumping dot with fixed amplitude, and eye movements were recorded for 59 subjects over two

recording sessions using an EyeLink 1000 eye tracking system with a sampling rate of 1000 Hz. The best reported result yielded an HTER of 19%.

Holland and Komogortsev [9] investigated individual and aggregated scanpath characteristics, representative of the brain's visual attention strategies during reading. Weighted mean fusion was employed to combine scores obtained by various characteristics. Eye movements were recorded for 32 subjects over four recording sessions using an EyeLink 1000 eye tracking system with a sampling rate of 1000 Hz. The best reported result yielded EER of 27%.

Komogortsev et al. [10] proposed to combine OPC and CEM modalities for the same reading stimulus and recording environment. When considered separately, OPC and CEM achieved HTER of approximately 27%; however, weighted fusion of the two provided an HTER of 19%, indicating a 30% improvement in accuracy.

Several areas that must be improved in eye movement related biometrics include: 1) size of available biometric databases; 2) cost of equipment; and, 3) biometric accuracy. The current work improves the state-of-the-art in these areas by: recording eye movements across 87 subjects, generating the largest available database for eye movement-based biometrics; the use of a single, low-cost image sensor, costing approximately \$20 in comparison to the commercial systems employed in previous research, which may cost \$5000-35000; and a resulting HTER of 33.6% provided by the combined eye movement-driven traits, an accuracy on par with previous findings.

2.2. Iris

2.2.1 Iris Biometrics on Low Cost Equipment

Lu et al. [11] modified a Sony Erickson P800 phone by adding an eye cap with custom-made lens and an IR light. The system was designed to capture grayscale iris images at the resolution of 640×480. The authors implemented Daugman's algorithm [12] on their mobile platform, and evaluation of the mobile algorithm with the CASIA-IrisV1 database was performed. FAR of 0.13-4.3% and FAR 0-8% was obtained, though the authors did not provide performance results using iris images captured by with the constructed device.

Thomas et al. [13] employed an Airlink SkyIPCam500W to capture 640×480 images in near infrared spectrum. The camera captured several images at the rate of 30 Hz. An LG IrisAccess system was employed for actual iris matching, and a small database of six subjects was used. The system was able to identify all users correctly and one additional person was correctly rejected as an imposter.

Sirohey et al. [14] located eye corners, eyelids, and irises in video data in order to determine changes in gaze direction and blinking, respectively. Considering the iris is always darker than the sclera, they started with segmentation of the scleric iris boundary. Then, anthropometric measures

bounded on the size of the iris relative to the size of the eye, and iris movements have limits imposed on them by the size of the eye. For eyelid edge, they used information about the eye corners and the iris center. The upper eyelid edge forms an arc that bounds the eye above the iris center. A flow-based method describes the movement of each component of the periocular region between frames, with respect to head motion, estimated by a flesh-tone color segmentation that gives a blob corresponding to the head.

Kai and Du [15] used a video sequence from the IUPUI data set and proposed an iris recognition strategy from low-level quality data. The iris is segmented by direct least square fitting, and a gradient-based strategy is applied locally to the segmented area to detect noise within the iris ring. Then, they proposed a two stage classification strategy, using information from different scales analyzed by SURF keypoint detection and Gabor filter decomposition.

Aiming to perform biometric iris recognition on low-quality video data, Jilela and Ross [16] fused information at the data-level in two stages: application of a so-called Principal Components Transform (PCT) to individual frames and averaging of the resulting images. The performance of image-level fusion was compared against that of score-level fusion, having authors observe significant improvements of the proposed technique, when compared to the use of any individual frame. Similarly, Hollingsworth et al. [17] took advantage of the temporal continuity in videos to improve matching performance using signal-level fusion. From multiple frames of a frontal iris video, they created a single average image, having observed that signal-level fusion performs comparably to state-of-the-art score-level fusion techniques, with less computation burden.

In summary, the iris capture setup employed in the current work is similar to existing studies; however, to the best of our knowledge, there is no research that combines iris and eye movement-driven biometric modalities. This work fills that gap by using a single image sensor to infer information about the iris and eye movements for biometric purposes.

2.2.2 Counterfeit Resistance

Recent studies report that existing iris-based biometric systems can be spoofed by simple replicas such as printed pictures of the iris [18]. There are also studies that propose quite sophisticated mechanisms for spoofing, e.g., semi-transparent contact lens [3]. As a result, there is a substantial body of work that describes aliveness and spoofing detection methods, e.g., [19, 20]; however, the race between ideas for iris spoofing and prevention methods primarily takes the route of manufacturing better material to represent the iris, and methods that detect non-human artifacts in that material [19].

We hypothesize that eye movement-related biometric methods that are driven by the sophisticated structure of the oculomotor plant and brain would be extremely effective in

rejecting intruders with iris replicas of even the highest possible quality. In that case, the accuracy of the underlying eye movement-driven method would determine the accuracy of fake iris rejection. The OPC and CEM methods discussed in this work can serve as a backbone for such counterfeit resistance mechanisms.

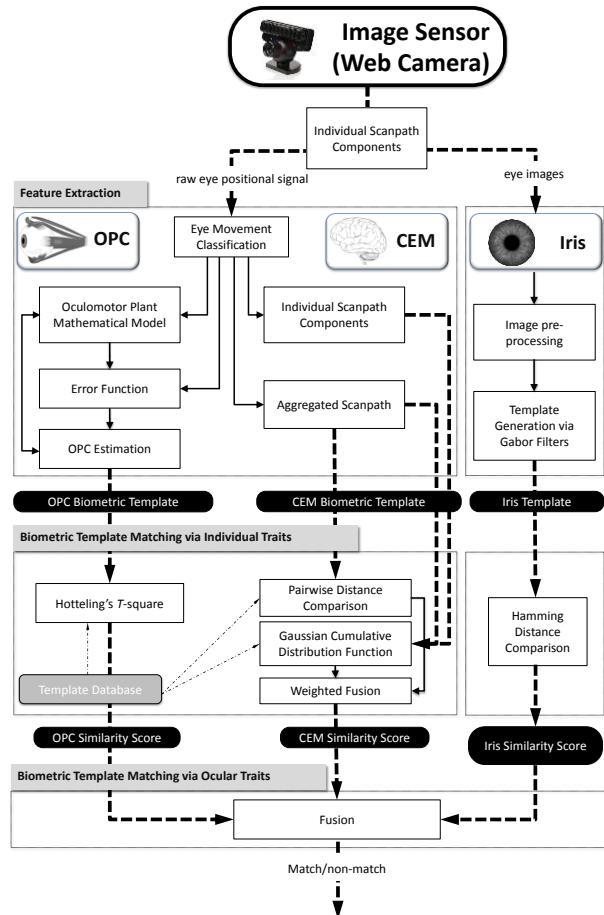


Figure 1: Multimodal ocular biometrics.

3. Multimodal Ocular Biometrics Approach

Three components comprise the multimodal ocular biometrics approach: 1) the internal, non-visible, anatomical structure of the human eye, represented by Oculomotor Plant Characteristics (OPC); 2) the visual attention strategies employed by the brain, represented by Complex Eye movement patterns (CEM); and, 3) the unique physical structure of the iris. All three traits may be derived from the same image stream, captured by a single camera sensor and driven by eye tracking software. Eye tracking software estimates the eye positional signal from the sequence of eye images, supplies this data to the OPC and CEM modules, and forwards images of the eye to the iris-processing module for subsequent generation of iris templates. Each module is capable of producing a comparison score that is fused into a single score for the final acceptance/rejection

decision. In the current implementation, scores are fused by a simple weighted sum approach. With all scores assigned as probabilities along the unit interval, normalization preceding fusion was unnecessary. Figure 1 depicts an overview of the proposed approach and the mechanics of each module.

3.1. Oculomotor Plant Characteristics (OPC)

The anatomy of the human eye provides a unique opportunity for biometric authentication, as there are a multitude of anatomical components that comprise the oculomotor plant (OP). These components include: the eye globe; the surrounding tissue and ligaments; six extraocular muscles (EOMs), each containing thin and thick filaments; tendon-like components; and various tissues and liquids [21]. The static and dynamic properties of the OP are represented by: the eye globe’s inertia; the force-velocity relationship of individual muscles; the resistive properties of the eye globe, muscles, and ligaments; the characteristics of the neuronal control signal, sent from the brain to the EOMs; and the speed of propagation of the neuronal control signal. Individual properties of the EOMs vary depending on their roles, which are two: agonist, representing the contracting muscle which pulls the eye globe; and antagonist, representing the lengthening muscle resisting the pull [22].

In this work, we employ a biometric method proposed by Komogortsev et al. [8]. In this method, a mathematical model of the eye simulated saccades and compares them to the recorded saccades extracted from the raw positional signal. Computed differences trigger OPC estimation procedures which attempt to find OPC values which minimize the difference in positional signal. Optimized OPC values form the biometric template.

Similar to the original method, we have selected the following nine OPC to form entries in the biometric template: length tension, series elasticity, passive viscosity of the eye globe, agonist force-velocity relationship, antagonist force-velocity relationship, tension intercept, and agonist and antagonist tension slopes [8]. The resulting template can be compared by Hotelling’s T-square test to another template, returning a probability score that can be employed to determine similarity.

3.2. Complex Eye Movement Patterns (CEM)

Complex Eye Movement patterns (CEM) represent the cognitive strategies employed by the brain throughout the guidance of visual attention. The human eye is connected to and controlled by a complex network of brain regions, sub-regions, and neural pathways [22, 23]. Information is transmitted from region to region along neural pathways in the form of neural signals, which may convey visual field information from the eye or control information from the brain. The firing rate of individual neural signals (which

occur in sustained bursts) is dependent on the physical properties of the involved neurons and surrounding brain tissue. As well, this neural activity is influenced by the task being performed, which may cause variation in baseline firing rates, firing rate profiles, and modulations of neuronal activity related to particular stimuli and behavioral responses [24].

We define fixation-based metrics as those metrics, which depend solely upon fixations and the mechanics involved in generating fixations. Fixation-based metrics include: fixation count (f_1) and average fixation duration (f_2). Fixation-based metrics involve and are dependent upon the: dorsal layers and rostral pole of the superior colliculus, nucleus raphe interpositus in the midline of the pons, posterior parietal cortex, and visual cortex areas V1-V5 [22, 23].

We define saccade-based metrics as those metrics, which depend solely upon saccades and the mechanics involved in generating saccades. Saccade-based metrics include: average vectorial saccade amplitude (f_3), average horizontal saccade amplitude (f_4), average vertical saccade amplitude (f_5), average vectorial saccade velocity (f_6), average vectorial saccade peak velocity (f_7), slope of the amplitude-duration relationship (f_8), slope of the main sequence relationship (f_9), and velocity waveform indicator (f_{10}). Saccade-based metrics involve and are dependent upon the: ventral layers of the superior colliculus, paramedian pontine reticular formation, rostral interstitial nucleus of the medial longitudinal fasciculus, frontal eye fields, and lateral intra parietal [22, 23].

We define scanpath-based metrics as those metrics which are derived from the size, shape, or pattern of the overall eye movement scanpath, and are often related to the visual search strategy employed in extracting information from a given stimuli. Scanpath-based metrics include: scanpath length (f_{11}), scanpath convex hull area (f_{12}), regions of interest (f_{13}), inflection count (f_{14}), and spatial distribution represented by a pairwise distance comparison (f_{15}). Scanpath-based metrics involve and are dependent upon the brain regions involved in fixation- and saccade-based metrics, as well as the conscious and sub-conscious memory mechanisms responsible for the guidance of visual search [25, 26].

Fixation and saccade related information is processed by the Individual Scanpath Components module and aggregated information is processed by the Aggregated Scanpath module. Components are combined by a weighted fusion method which outputs a single similarity score for a given pair of CEM templates. Additional details are provided elsewhere [9].

3.3. Iris

Considering the specific characteristics of iris data, it is especially important to define an initial region of interest,

from which subsequent processing occurs. The near infrared (NIR) structured light guarantees maximum contrast between the pupil and any remaining data. Hence, the first step comprises the detection of a bounding box that contains the pupil, made according to orthogonal projections. Then, a first order gradient-based edge detection [27] feeds a circular Hough transform phase, yielding the parameterized papillary boundary. Morphological constraints are especially useful to constrain the potential regions of search for the scleric boundary, accomplished in a similar way to the inner boundary. The translation into the Polar domain gives rough invariance to changes in scale. An optimal Gabor filter [12] configuration (wavelength: $1/4$, orientation $5\pi/8$, phase offset: 0, sigma Gaussian: $1/8$, spatial aspect ratio: 1) is selected to extract the iris biometric template¹. Template matching is performed in angularly constrained regions of the normalized data, where eyelid and eyelash occlusions are less probable. As a result of template matching, a distance score is returned by the iris module. The score can be employed in the similarity decision. It should be stressed that more elaborate segmentation/encoding strategies were not considered, due to the limited resolution of obtained iris data.

4. Experimental Setup

4.1. Equipment & Software

Eye movement recording and iris capture were simultaneously conducted using a PlayStation Eye web camera (approximate cost of \$20). The camera recorded at the resolution of 640×480 pixels with a frame rate of 75 Hz. The existing IR filter was removed and a piece of unexposed film was inserted as a filter for the visible spectrum of light. A Clover Electronics IR010 Infrared Illuminator (approximate cost of \$33) and two IR diodes (approximate cost of \$2) placed on the body of the camera were employed to improve the quality of iris illumination and eye tracking accuracy. The web camera and main IR array were each installed on the flexible arm of a Mainstays Halogen Desk Lamp (total approximate cost \$20) to provide an installation that can be adjusted to specific users. A chin rest (readily available from a commercial eye tracking system) was employed for head stabilization to improve the quality of acquired data. In a low-cost scenario, a comfortable chinrest can be constructed from very inexpensive materials.

The stimulus was displayed on a 19-inch LCD monitor with a refresh rate of 60 Hz. The distance between the eye and the screen was approximately 540 mm.

ITU Gaze Tracker [28], publicly available eye tracking software, was employed for eye tracking purposes. The

¹ Optimal parameters were selected based on analysis of the training dataset.

software was modified to present the required stimuli and store an eye image every three seconds, in addition to the existing eye tracking capabilities. Eye tracking was done in no-glint mode. Duchowski provides an overview of general eye tracking principles [23].

4.2. Stimulus

A complex pattern stimulus was constructed that employed the Rorschach inkblots commonly used in psychological examination [29], in order to provide relatively clean patterns which were likely to evoke varied thoughts and emotions in participants. Inkblot images were selected from the original Rorschach psychodiagnostic plates and sized/cropped to fill the screen. Participants were instructed to examine the images carefully, and recordings were performed over two sessions, with 3 rotations of 5 inkblots per session. Each inkblot was displayed for 12 sec, for a total of 3 min per session.

4.3. Participants & Data Collection

Eye movement and iris data was collected for a total of 87 subjects (60 male, 27 female), ages 18 – 47 with an average age of 22.6 (SD = 4.8). An Institutional Review Board approved data collection procedures, and all subjects provided informed consent. Each subject participated in two recording sessions with an interval of approximately 15 min between sessions.

During the data collection phase, the recording facilitators were instructed to adjust the equipment to provide high quality eye movement data and iris images. The quality of the eye movement data was controlled by the magnitude of calibration error. The facilitators were instructed to adjust the equipment to keep this error under 2° of the visual angle for any participant. The quality of iris images was controlled by visual inspection that targeted iris diameter in a range of 100 pixels, was in focus, with iris pattern clearly visible. In cases where maintaining high quality eye movement data and iris images at the same time was not possible, the preference in quality was given to the eye movement data. This scenario happened for several subjects, for whom high quality iris images degraded the performance of the eye tracking software. Figure 2 provides an example eye movement scanpath collected from a single subject/inkblot, and Figure 3 provides examples of collected iris quality.

4.4. Datasets & Data Quality

Across all eye movement recordings, mean positional accuracy represented by the magnitude of calibration error was 1.06° (SD = 0.64°). For each recording session, one best iris image was selected manually to provide a one-to-one correspondence between related OPC, CEM, and iris templates. Captured iris images had mean diameter

of 103.3 pixels (SD = 22 pixels). Mean focus score computed by eq. 15 in [30] was 75 (SD = 24.7). For comparison, the ICE 2005 iris dataset [31] has mean focus score of 163 (SD = 27.5).

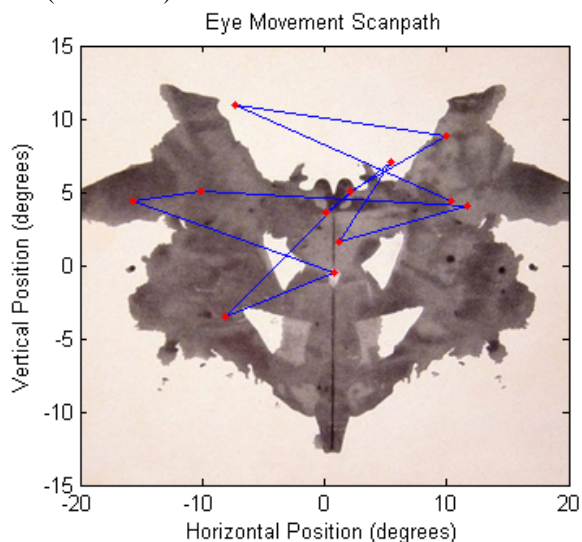


Figure 2: Example scanpath.



Figure 3: Example iris quality. Left image: poor quality. Middle image: acceptable quality. Right image: good quality.

5. Results

Results are presented in Figure 4 and Table 1.

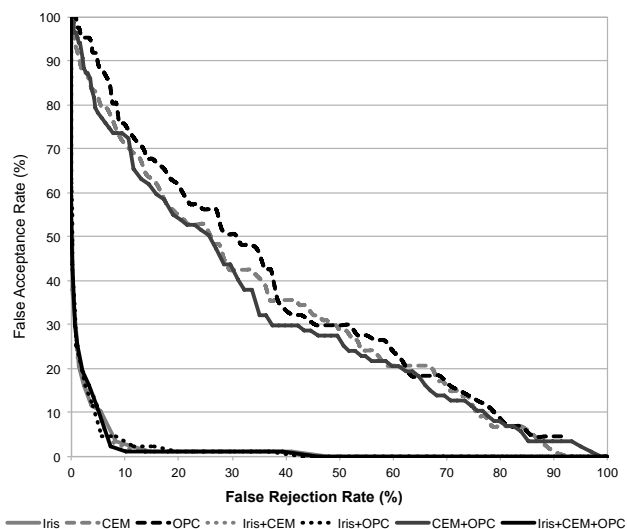


Figure 4: Detection error tradeoff. “+” sign indicates weighted fusion with weights presented in Table 1.

Table 1. Decidability index and HTER for each method. Decidability index is computed by eq. 14 in [30]. HTER computed as $(FAR+FRR)/2$ is derived from the data points that are as close as possible to the interpolated EER. OPC_h and OPC_v represent the scores obtained from the horizontal and vertical movement components respectively. Features related to CEM were identified in Section 3.1.

Method Name	Decidability Index	HTER
OPC h	0.35	41.7
OPC_v	0.39	40.5
OPC = $0.53*OPC_h+0.47*OPC_v$	0.5	37.1
CEM = $0.009*f_4+0.037*f_5+0.917*f_7+$ $+f_{11}*0.037$	0.58	36.3
Iris	3.07	5.9
$0.98*Iris+0.02*OPC$	3.09	5.1
$0.98*Iris+0.02*CEM$	3.08	5.7
$0.37*OPC+0.63*CEM$	0.68	33.6
$0.02*OPC+0.02*CEM+0.96*Iris$	3.1	4.8

5.1. Oculomotor Plant Characteristics (OPC)

HTER provided by OPC alone was 37.1%, much higher than the comparable result of 22.5% reported in [8]. The 65% increase in error is not unexpected considering a significant reduction in sampling frequency (75 Hz vs. 1000 Hz). We hypothesize that equipment precision (the minimum distance the eye should move before a shift in position is detected) is much lower on the web camera based eye tracker, which contributes to the increase in error. Consider the web camera eye tracker is approximately three orders of magnitude less expensive than commercial equipment, it is important to notice that OPC performance is still far from the random baseline.

5.2. Complex Eye Movement Patterns (CEM)

HTER provided by CEM alone was 36.3%, which is higher than the comparable result of 27% reported in [9]. We hypothesize this 34.4% increase in error is due to reduction in sampling rate and equipment precision. It is possible to notice that the increase in CEM error is much smaller than the increase in OPC error. There are two points to consider: 1) accurate estimation of the OPC may require a low-noise, accurate signal and high sampling rate; 2) initial error of 27% reported for CEM in [9] is higher than the error of 22.5% reported for OPC in [8]. Therefore, it is possible to make the preliminary conclusion that OPC provides better verification than CEM on higher accuracy and sampling rate equipment; however, CEM is more tolerant to accuracy and sampling rate degradation than OPC.

5.3. Iris

Considering the demands given by ISO/IEC 19794-6 (“an iris diameter of more than 200 pixels is considered to be good”), the average dimension of the iris rings in the acquired are far below that value. Unavoidably, this gap in the amount of information should correspond to an increase in the observed error rates of the iris recognition model. Not surprisingly, we observed that the optimal Gabor configuration was obtained at shorter wavelengths than those obtained for more usual datasets of iris recognition experiments (e.g. the ICE dataset), yielding HTER values around 5.9%. These allowed us to conclude that even in such challenging data, iris rings contain discriminating information, with potential to be used for biometric recognition purposes. Additionally, we empirically observed that slight increases in the amount of information acquired correspond to substantial improvements in iris recognition performance.

5.4. OPC + CEM

Combining OPC and CEM increased the accuracy of the verification, yielding an HTER of 33.6%. This constitutes a 9.4% reduction in error compared to OPC and a 7.4% reduction in error compared to CEM. The magnitude of error reduction is smaller than the 30% reported by Komogortsev et al. [10]; however, it is still substantial.

5.5. OPC + CEM + Iris

Fusion of OPC and iris traits reduced error by 13.4% when compared to iris modality alone, and fusion of CEM and iris traits reduced error by 3.4% when compared to iris modality alone. The combination of OPC, CEM, and iris traits provided an error reduction of 19% when compared to the iris modality alone. This reduction in error is quite substantial, indicating high potential for the combined ocular biometrics approach on low-cost equipment.

6. Discussion

6.1. Counterfeit Resistance

The best HTER achieved by CEM and OPC modalities is 33.6%, quite high when compared to the 0% error rate for the detection of contact lens reported by He et al. [32]. Eye movement biometrics still has a long way to go in terms of accuracy; however, we hypothesize that in a race between the artifact and detection mechanisms, eye movement driven methods may provide more robust solutions in the long run.

6.2. Limitations

There are several limitations in this study. First, subjects did not move their heads during recording, which is unre-

alistic during normal computer use. Second, weights for the weighted fusion and thresholding were selected for the dataset as a whole, similar to [8-10]. Third, eye images for iris recognition were selected manually; however, it is not difficult to imagine automated mechanisms that would perform such selection automatically (e.g. [33]). Fourth, only a single eye image per recording was selected for iris recognition purposes. Possible employment of a larger range of images, similar to [16], may improve iris related accuracy. Fifth, both recording sessions were done in close temporal proximity, therefore negating possible impacts related to fatigue, illness, or drug consumption. The impact of these factors over a longer recording timeline should be investigated in future work.

7. Conclusion and Future Work

The current work proposed a multimodal ocular biometric approach that combines three physiological and behavioral traits related to Oculomotor Plant Characteristics (OPC), Complex Eye Movement patterns (CEM), and iris patterns. The results indicate that it is possible to extract biometric information encoded in those traits using a single image sensor. The image sensor employed in our study was an inexpensive web camera, which contrasts with previous eye movement-driven studies that employed high-quality, commercial eye tracking equipment. As a result, the largest existing database of eye movements and corresponding iris images of 87 people was recorded and will be publicly available.

From the eye movement-driven biometric perspective, our results support findings reported in previous research and indicate that OPC and CEM are able to provide some information about biometric identity even when using inexpensive image sensors.

From the iris biometrics perspective, we confirm that: 1) it is possible to achieve reasonably low error rates (HTER = 5.6%) when operating on data with resolution substantially lower than ISO/IEC 19794-6 recommendations; and 2) the discriminating information of the iris texture correlates weakly to eye movement-driven biometric sources, which makes it possible to strengthen biometric accuracy by combining information from these traits. As a result, when compared to iris authentication alone, the multimodal ocular biometric provided an error reduction of 19%, with a resulting HTER = 4.8%.

We hypothesize that eye movement-driven biometrics can serve as a complimentary method for liveness and spoofing detection to already existing mechanisms in future biometric systems. We plan to address this issue in detail in our future work.

8. Acknowledgment

This work was supported in part by the National Institute of Standards and Technology (NIST) under Grant

#60NANB10D213, the National Science Foundation (NSF) under Grant #DGE-11444666, and Texas State University-San Marcos via internal grants.

References

- [1] A. A. Ross, K. Nandakumar and A. K. Jain. Handbook of multibiometrics. Springer, 2006.
- [2] Available: <http://cw.com.hk/news/report-hong-kong-china-border-bio-metrics-device-spoofed>.
- [3] N. B. Puhan, S. Natarajan and A. Suhas Hegde. Iris liveness detection for semi-transparent contact lens spoofing advances in digital image processing and information technology. Springer Berlin Heidelberg, 249-256, 2011.
- [4] P. Kasprowski and J. Ober. Eye movements in biometrics. Proceedings of the European Conference on Computer Vision (ECCV), 248-258, 2004.
- [5] P. Kasprowski and J. Ober. Enhancing eye-movement-based biometric identification method by using voting classifiers. Proceedings of 314-323, 2005.
- [6] R. Bednarik, T. Kinnunen, A. Mihaila and P. Fränti. Eye-movements as a biometric. Image analysis, 780-789, 2005.
- [7] I. Rigas, G. Economou and S. Fotopoulos. Biometric identification based on the eye movements and graph matching techniques. Pattern Recognition Letters, 33(6):786-792, 2012.
- [8] O. V. Komogortsev, A. Karpov, L. Price and C. Aragon. Biometric authentication via oculomotor plant characteristic. Proceedings of IEEE/IARP International Conference on Biometrics (ICB), 1-8, downloaded at <http://www.cs.txstate.edu/~ok11/publications.html> 2012.
- [9] C. Holland and O. V. Komogortsev. Biometric identification via eye movement scanpaths in reading. Proceedings of 1-8, 2011.
- [10] O. V. Komogortsev, A. Karpov and C. Holland. Cue: Counterfeit-resistant usable eye-based authentication via oculomotor plant characteristics and complex eye movement patterns. Proceedings of SPIE Defence Security+Sensing Conference on Biometric Technology for Human Identification IX, 1-10, downloaded at <http://www.cs.txstate.edu/~ok11/publications.html> 2012.
- [11] H. Lu, R. C. D. Young and C. R. Chatwin. Iris recognition on low computational. Power mobile devices. Biometrics - unique and diverse applications in nature, science, and technology, 106-127, 2011.
- [12] J. G. Daugman. Complete discrete 2-d gabor transforms by neural networks for image analysis and compression. Acoustics, Speech and Signal Processing, IEEE Transactions on, 36(7):1169-1179, 1988.
- [13] N. L. Thomas, Y. Du, S. Muttineni, S. Mang and D. Sran. Low-cost mobile video-based iris recognition for small databases. Proceedings of 73510D-73517, 2009.
- [14] S. Sirohey, A. Rosenfeld and Z. Duric. A method of detecting and tracking irises and eyelids in video. Pattern Recognition, 35(6):1389-1401, 2002.
- [15] Y. Kai and E. Y. Du. A multi-stage approach for non-cooperative iris recognition. Proceedings of Systems, Man, and Cybernetics (SMC), 2011 IEEE International Conference on, 3386-3391, 2011.
- [16] R. Jillela, A. Ross and P. J. Flynn. Information fusion in low-resolution iris videos using principal components transform. Proceedings of Applications of Computer Vision (WACV), 2011 IEEE Workshop on, 262-269, 2011.
- [17] K. Hollingsworth, T. Peters, K. W. Bowyer and P. J. Flynn. Iris recognition using signal-level fusion of frames from video. Information Forensics and Security, IEEE Transactions on, 4(4):837-848, 2009.
- [18] Available: http://www.theregister.co.uk/2002/05/23/biometric_sensors_beaten_senseless/.
- [19] P. Andrzej and C. Adam. Aliveness detection for iris biometrics. Proceedings of Carnahan Conferences Security Technology, Proceedings 2006 40th Annual IEEE International, 122-129, 2006.
- [20] X. He, Y. Lu and P. Shi. A new fake iris detection method. Proceedings of the Third International Conference on Advances in Biometrics, Springer-Verlag, 1132-1139, 2009.
- [21] D. R. Wilkie. Muscle. London: Arnold, 1970.
- [22] R. J. Leigh and D. S. Zee. The neurology of eye movements. Oxford University Press, 2006.
- [23] A. T. Duchowski. Eye tracking methodology: Theory and practice. Springer-Verlag, 1-360, 2007.
- [24] W. F. Asaad, G. Rainer and E. K. Miller. Task-specific neural activity in the primate prefrontal cortex. Journal of Neurophysiology, 84(1):451-459, 2000.
- [25] D. Noton and L. W. Stark. Scanpaths in eye movements during pattern perception. Science, 171(3968):308-311, 1971.
- [26] T. Ro, J. Pratt and R. D. Rafal. Inhibition of return in saccadic eye movements. Experimental Brain Research, 130(2):264-268, 2000.
- [27] J. Canny. A computational approach to edge detection. Pattern Analysis and Machine Intelligence, IEEE Transactions on, PAMI-8(6):679-698, 1986.
- [28] J. S. Agustin, H. Skovsgaard, E. Mollenbach, M. Barret, M. Tall, D. W. Hansen and J. P. Hansen. Evaluation of a low-cost open-source gaze tracker. Proceedings of Proceedings of the ACM Symposium on Eye-Tracking Research & Applications (ETRA), 77-80, 2010.
- [29] H. Rorschach. Rorschach test - psychodiagnostic plates. Hogrefe, 1-10, 1927.
- [30] J. Daugman. How iris recognition works. IEEE Transactions on Circuits and Systems for Video Technology, 14(1):21-30, 2004.
- [31] Available: <http://www.nist.gov/itl/iad/ig/ice.cfm>.
- [32] X. He, S. An and P. Shi. Statistical texture analysis-based approach for fake iris detection using support vector machines advances in biometrics. Springer Berlin / Heidelberg, 540-546, 2007.
- [33] Y. Lee, R. J. Micheals and P. J. Phillips. Improvements in video-based automated system for iris recognition (vasir). Proceedings of Proceedings of the IEEE international conference on motion and video computing, 71-78, 2009.